Ultrafast Reactivity of IR-Excited Electron in Aqueous Ionic Solutions

Y. Gauduel,* M. Sander,† and H. Gelabert

Laboratoire d'Optique Appliquée, CNRS UMR 7639, INSERM U451, ENS Techniques Avancées, Ecole Polytechnique, 91761 Palaiseau cedex, France

Received: January 16, 1998

An ultrafast presolvation reaction involving IR-excited hydrated electrons and bivalent metal cations $(Cd^{2+})_{aq}$ was investigated at the femtosecond time scale. The initial electron photodetachment is triggered by a two-photon UV excitation of aqueous chloride ions ($R = [H_2O]/[XCl_2] = 110$). The photodetached electron reaches a IR p-like state (prehydrated electron) with a time constant of 130 fs at 294 K. In the presence of nonreactive divalent alkaline metal cations ($X^{2+} = Mg^{2+}$), this transient IR electronic state exhibits a deactivation process toward the ground state of hydrated electron (s state) with a time constant of 300 ± 20 fs. In aqueous $CdCl_2$ solution, an ultrafast IR electron transfer channel (univalent reduction of Cd^{2+} by IR prehydrated electrons) competes with the p → s transition of trapped electrons (electron solvation process). This presolvation reaction occurs with a characteristic time of 140 ± 20 fs. Within the electron solvation regime, this elementary redox process is totally achieved in less than 1×10^{-12} s and exhibits a probability 10 times higher than the electron hydration channel. The consequence of an early partition between reactive and nonreactive IR electron dynamics on the subpicosecond formation of fully hydrated electron is discussed. The femtosecond IR spectroscopy of excited p-state electron transfer processes in aqueous electrolyte solutions opens a new area of prethermal reactions in environments relevant to mainstream chemistry and biochemistry.

1. Introduction

Fundamental investigations on electron transfer and reaction dynamics in solutions are progressing with recent advances of ultrafast spectroscopies and computational chemistry.[1−12] The course of elementary redox reactions may be observable on the time scale of molecular motions, and some important aspects concern the dynamical response of a molecular solvent to a sudden change in the charge distribution of a solute or a transition state immersed in it.[13−21] At a potential energy surfaces crossing zone that couples the coordinate motion of an electron transfer reaction with an electron solvation process, microscopic nonequilibrium effects can assist or impede early electron transfer steps and affect branchings between nonequilibrium electronic trajectories. Significant advances in the understanding of redox and radical reactions in solutions require the real-time discrimination between nonreactive and reactive electron dynamics.

During the past decade, numerous aspects of the dynamical properties of liquid water have been explored[22−28] and major experimental strides have been performed in solvation dynamics of molecular probes[17−19,29,30] and excess electron.[31,34] In synergy with semiquantum nonadiabatic molecular dynamics simulations,[10,35−37] femtosecond IR discrimination of a nonequilibrium electron (p-like state of excited solvated electron) in pure water,[31,32,38] aqueous organized assemblies,[39] and ionic solutions[40−42] are beginning to provide a detailed picture of an elementary radical solvation. Regarding the p → s transition of an excess electron in a polar liquid, dynamical cage effects are largely dependent on statistical properties of solvent molecules, solute reorientational dynamics, and fluctuations of solute−solvent electronic polarizability, and the role of translational solvent motions is more and more emphasized.[36,37]

In polar solutions, intermolecular electron transfer faster than the picosecond solvation process has been investigated by fluorescence up-conversion[43−44] but up to now competitive nonreactive electron dynamics (electron solvation) and ultrafast presolvation radical reactions in water have not be investigated at very short times. Nanosecond and picosecond pulse radiolysis studies have suggested that ultrafast radical reaction (univalent reduction of a solute) would involve hot electrons or short-lived precursors of hydrated electron.[45−51] These indirect investigations determine the subnanosecond *G* value of solvated electrons for different electron scavenger concentrations. The pulse radiolysis experiments treat the data by determining empirical relationships between the rate constant of an electron transfer and the C_{37} value,[47−49] or stochastic analysis of competitive electron solvation and electron capture.[50] The investigations of ultrafast electron transfers at the macroscopic level do not permit one (i) to understand in detail presolvation intermolecular charge transfer, and (ii) to determine the exact nature of early branching between short-lived nonreactive and reactive electronic configurations. Some important aspects would concern the influence of ultrashort-lived solvent configurations on the probability of curve crossing. How does a molecular solvent modify the probability of curve crossing during a nonadiabatic electron transfer? Can an ultrafast reduction reaction involve short-lived couplings between trapped electrons and nonequilibrium water molecules configurations? Dynamical solvent cage effects can be governed by librational motions, short-range polarization, vibronic effects, and reorientational correlation function of solvent molecules in the vicinity of newly created electronic configurations. Aqueous electrolyte solutions represent a paradigm for the investigation of ultrafast presolvation redox reactions in environments relevant to mainstream chemistry and biochemistry. Femtosecond UV−IR spectroscopy of electron dynamics allows one to study early partitions between

* Author to whom correspondence should be addressed. Phone: +33-(0)1 69 31 97 26. Fax: +33(0)1 69 31 99 96. E-mail: gauduel@enstay.ensta.fr.

† Permanent address: Institut für Physikalische Chemie, Universität Göttingen, 37085 Göttingen, Germany.

S1089-5639(98)00804-4 CCC: $15.00
Published on Web 09/12/1998

short-lived electron transfer trajectories and to investigate the role of inhomogeneous microscopic structures on elementary redox reactions.

The present paper is mainly focused on the femtosecond IR spectroscopy of ultrafast presolvation electron reaction in aqueous electrolyte solutions. We report the short-time reduction of a bivalent metal cation (Cd^{2+}) by IR prehydrated electrons (eq 1a). This ultrafast prehydration univalent reduction

$$\{Cl^- + Cd^{2+}\}_{aq} \xrightarrow{2h\nu}$$

$$\left(\begin{matrix}\text{excited}\\ \text{states}\end{matrix}\right) \xrightarrow{T_1} \{Cl + Cd^{2+}\}_{aq} + \{e^-_{IR}\}_{Reac} \xrightarrow[T_{Reac}]{\begin{matrix}\text{prehydration}\\ \text{reduction}\end{matrix}} \{Cl + Cd^{+}\}_{aq} \qquad (1a)$$

$$\downarrow T_1'$$

$$\{Cl + Cd^{2+}\}_{aq} + \{e^-_{IR}\}_p \rightarrow s \xrightarrow[T_2]{\begin{matrix}\text{electron}\\ \text{hydration}\end{matrix}} \{Cl + Cd^{2+}\}_{aq} + e^-_s \qquad (1b)$$

of Cd^{2+} competes with an electron solvation channel which is linked to a p → s transition of IR prehydrated electrons (eq 1b). The consequence of an early partition between reactive and nonreactive electron dynamics on the subpicosecond formation of solvated electrons is also discussed.

2. Experimental Section

Elementary electron transfers from aqueous halides ions (Cl^-) are triggered by a two-photon excitation process with femtosecond UV laser pulses (4 eV). The colliding pulse mode-locked laser followed by five amplifier stages has been discussed previously.[52] The compression of amplified beams through a four-prism arrangment allows output pulses of energy above 1 mJ and typically of 80−90 fs duration at a 20 Hz repetition rate. The pump beam is generated by frequency doubling of amplified pulses in a 1 mm KDP crystal and focused on a quartz Suprasil cell. In the sample, pump and probe beams overlap on less than 0.5 mm. For the time-resolved IR spectroscopy, the energy of the excitation pulse is adjusted at 7 ± 0.5 μJ and the test beam is selected from a continuum generation with thin optical filters. The time dependence of induced IR absorption signals is investigated with germanium photodiodes. The different procedures that we use to analyze femtosecond IR spectroscopic data on aqueous ionic solutions have been published in recent papers.[42] The computational analysis of femtosecond IR spectroscopic data were performed on a Sun Sparcstation. Aqueous salt solutions at 294 K were produced by dissolving magnesium chloride (purity 99.999%) or cadmium chloride (purity 99.999%) from Aldrich Chemical Co in light water at a final concentration of 0.5 M. This concentration corresponds to a molecular ratio R of 110 ($R = [H_2O]/[XCl_2]$, X = Mg, Cd). Water is bidistilled in a quartz distillator with $KMnO_4$ and its resistivity is greater than 19 MΩ at 294 K. In order to avoid undesirable oxidative processes in the sample, molecular oxygen was removed by using pure nitrogen gas flow.

3. Results and Discussion

3.1. Femtosecond IR Spectroscopy of Aqueous XCl_2 Solutions (X = Mg, Cd). Aqueous magnesium chloride solutions are used for the investigation of ultrafast nonreactive IR electron dynamics and the comparison with prehydration electron transfers on reactive bivalent metal cations (Cd^{2+}). The IR spectroscopic data on early two-photon-induced electron transfer processes are reported in Figure 1 and Table 1. The quantitative analysis of IR spectroscopic data were performed

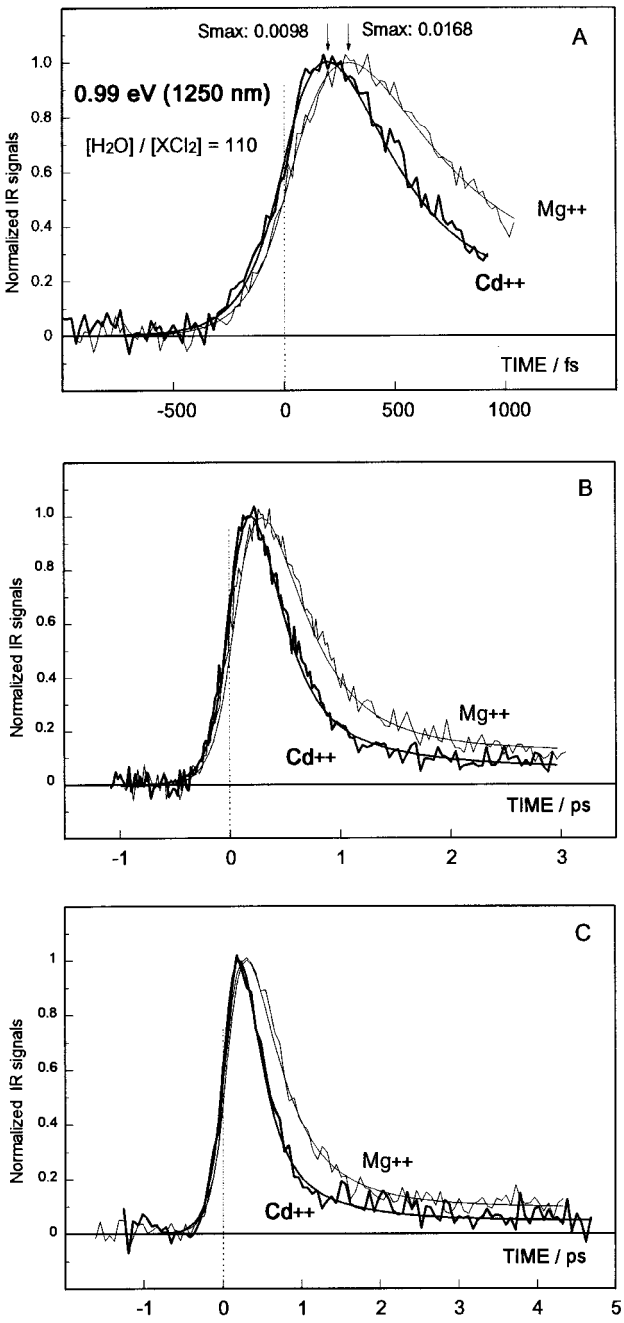

Figure 1. Infrared spectroscopy of ultrafast one-electron reduction of aqueous cadmium ions (Cd^{2+}) by IR p-state prehydrated electrons at 294 K ($[H_2O]/[CdCl_2] = 110$). The reference solution contains a nonreactive cation ($[H_2O]/[MgCl_2] = 110$). Smooth lines represent the best computed fits of nonexponential IR signal decays at 0.99 eV. In $MgCl_2$ solutions, the IR signal decay is expressed by the prevailing p → s transition of prehydrated electron (0.7 exp(−t/0.3) and two minor contributions of CTTS** (0.14 exp(−t/0.05) and {Cl:e^-}pairs (0.09 exp(−t/0.33). In $CdCl_2$ solutions, the prehydration redox reaction with $\{e^-_{IR}\}_{Reac}$ contributes to the prevailing IR decay (0.71 exp(−t/0.14). Minor electronic channels (0.10 exp(−t/0.05) + (0.07 exp(−t/0.3) + 0.08 exp(−t/0.33)) correspond to CTTS**, $\{e^-_{IR}\}_{p\rightarrow s}$, and {Cl:$e^-$}pairs, respectively. The incomplete recovery of IR signal is due to the low-energy tail contribution of the hydrated electron ground state (e^-_s).

for different time windows (2, 4, and 6 ps). In aqueous $MgCl_2$ solutions ($R = [H_2O]/[MgCl_2] = 110$), the prevailing IR electronic trajectory involves an electron photodetachment from excited states of chloride ion and the formation of a precursor of the hydrated electron ($\{e^-_{IR}\}$ or $\{e^-_{Hyd}*\}$) with a characteristic time T_1 of 130 fs (eq 2a). This excited p-state of the

TABLE 1: Effects of Aqueous Divalent Metal Cations (Mg^{2+}, Cd^{2+}) on the IR Electron Dynamics, and Early Partition between a Presolvation Reduction Reaction (Eq 1a) and an Electron Hydration Channel (Eq 1b)[a]

parameters	$[H_2O]/[MgCl_2] = 110$	$[H_2O]/[CdCl_2] = 110$
T_1 (fs)	130 ± 10	130 ± 10
T_1' (fs)		130 ± 10
T_2 (fs)	300 ± 20	300 ± 20
T_{Reac}		140 ± 20
$P_{p\rightarrow s}$	1	0.09
P_{Reac}	0	0.91
$P_{Reac}/P_{p\rightarrow s}$	0	10.1

[a] In aqueous $CdCl_2$ solution, the parameters are calculated from a kinetic model presented in Figure 3A.

hydrated electron relaxes toward the ground state of hydrated electron with $T_2 = 300$ fs. The relative spectral contribution of this IR state ($\alpha_{\{e^-\}IR}$) equals 0.70 (Figure 1). In comparison with previous femtosecond spectroscopy of electron dynamics in aqueous sodium chloride solutions,[42,52] the time dependence of IR absorption signal is not significantly modified by the presence of a divalent counterion (Mg^{2+}). This electronic relaxation channel represents the main electron solvation process that occurs in the water bulk.[42,54] The low-energy tail of the hydrated electron ground state contributes to the incomplete recovery of the IR signal.

$$Cl^-_{aq} + 2h\nu \rightarrow (\text{excited states}) \xrightarrow{T_1 = 130\ \text{fs}} e^{-1}_{IR} + Cl_{aq} \xrightarrow{T_2 = 300\ \text{fs}} e^-_s + Cl_{aq} \quad (2a)$$

$$Cl^-_{aq} + 2h\nu \xrightarrow{t \ll 50\ \text{fs}} CTTS^{**} \xrightarrow{t \sim 50\ \text{fs}} CTTS^{*} \quad (2b)$$

$$Cl^-_{aq} + 2h\nu \xrightarrow{t = 270\ \text{fs}} (Cl{:}e^-)_{aq} \xrightarrow{t = 330\ \text{fs}} Cl^-_{aq} \quad (2c)$$

Two minor electronic channels assigned to excited CTTS states (CTTS**) and electron−atom pairs contribute to the nonexponential IR signal decay observed at 0.99 eV (eq 2b,c). The spectral contributions of these transient states represent 20% of the subpicosecond IR signal (Figure 1). They exhibit the same dynamics as those previously investigated in aqueous NaCl solutions.[52,53]

Data on femtosecond IR spectroscopy of aqueous cadmium chloride solutions are presented in Figures 1 and 2. The experimental curves discriminated for different temporal windows (2−6 ps) underline a significant Cd^{2+} effect on the IR signal dynamics. For the same molecular ratio ($[H_2O]/[XCl_2] = 110$), the substitution of Mg^{2+} by Cd^{2+} lowers the IR signal amplitude (S_{max}) and shortens the absorption signal rise time. Indeed, within a very short time window (2 ps) the spectroscopic data emphasize that S_{max} (0.99 eV) is obtained for $\tau = 300$ fs with Mg^{2+} and $\tau = 200$ fs with Cd^{2+}. Simultaneously, the amplitude of the IR signal is decreased by 40−45% in aqueous $CdCl_2$ solution (Figure 2A).

3.2. Kinetic Model of a Presolvation Reduction Reaction in Aqueous $CdCl_2$ Solution. In aqueous $CdCl_2$ solutions, the kinetic model investigates the influence of reactive trajectories on the dynamics and amplitude of the IR absorption signal (Figure 3). We have focused our attention on (i) the prevailing trajectory of IR prehydrated electrons, and (ii) the role of early branchings between reactive (eq 1a) and nonreactive (eq 1b) channels. Due to the low C_{37} value of aqueous Cd^{2+},[50] the computed kinetic model investigates a prehydration one-electron reduction of Cd^{2+}. This ultrafast redox channel would be triggered by an electron photodetachment from excited aqueous

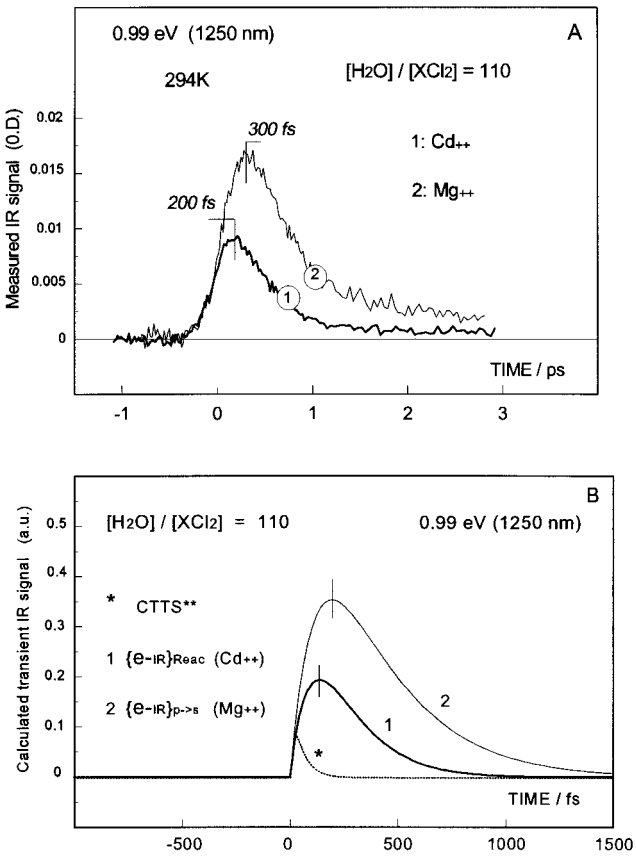

Figure 2. (A) Time dependence of measured IR absorption signal amplitudes (OD) following the femtosecond UV excitation of aqueous chloride ions in $MgCl_2$ or $CdCl_2$ solutions. (B) Calculated effect of an ultrafast prehydration one-electron reduction of Cd^{2+} ions on the transient level of reactive ($\{e^-_{IR}\}_{Reac}$) and non-reactive ($\{e^-_{IR}\}_{p\rightarrow s}$) trajectories. The transient level of very short-lived CTTS** is also represented.

chloride ions with a probability P_{Reac} (eq 3). In this expression, β_p represents the absorption coefficient for a two-photon excitation process of the halide ion. The ultrafast prehydration electron transfer on Cd^{2+} is characterized by the time constant T_{Reac} (eq 4) and includes the reactivity of transient IR presolvated electron $(e^-_{IR})_{Reac}$.

$$\frac{dn_1^*}{dt} = P_{Reac}\beta_P\frac{I_P^2}{2h\omega_P} - \frac{n_1^*}{T_1'} \quad (3)$$

$$\frac{dn_{(e^-_{IR})_{Reac}}}{dt} = \frac{n_1^*}{T_1'} - \frac{n_{(e-IR)Reac}}{T_{Reac}} \quad (4)$$

This ultrafast one-electron reduction of Cd^{2+} induces an early partition between a reactive electron photodetachment channel and the nonreactive electron hydration channel. The contribution of an IR electron solvation channel leading to the ground state of hydrated electron is characterized by the probability $P_{p\rightarrow s} = 1 - P_{Reac}$ (eqs 5 and 6):

$$\frac{dn_2^*}{dt} = (1 - P_{Reac})\beta_P\frac{I_P^2}{2h\omega_P} - \frac{n_2^*}{T_1} \quad (5)$$

$$\frac{dn_{(e^-_{IR})_{p\rightarrow s}}}{dt} = \frac{n_2^*}{T_1} - \frac{n_{(e-IR)p\rightarrow s}}{T_2} \quad (6)$$

As in aqueous $MgCl_2$ solutions, T_1 and T_2 represent the trapping

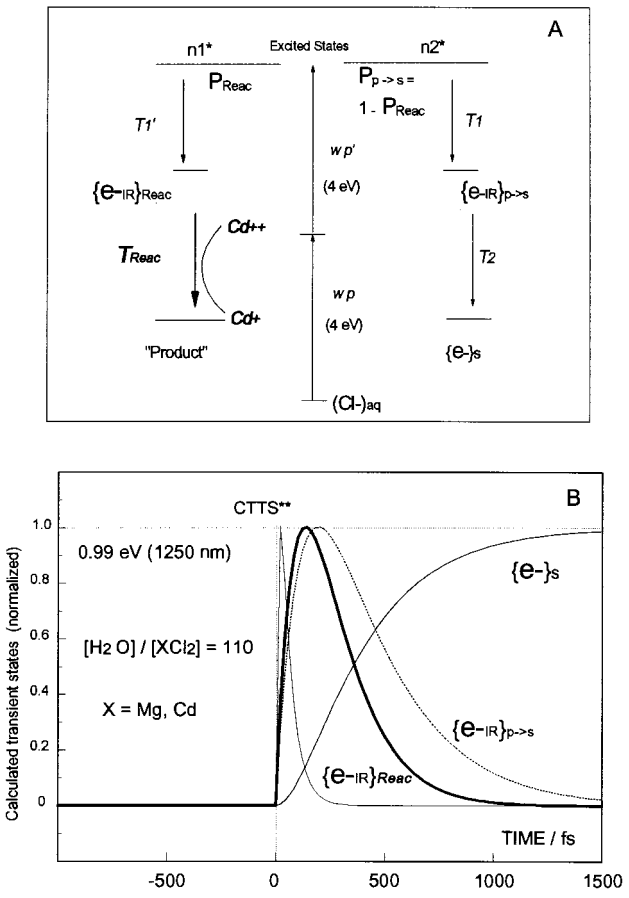

Figure 3. (A) Kinetic model used for the analysis of ultrafast infrared electrons dynamics in presence of aqueous cadmium ion. This model considers the existence of an early partition between a p → s transition of hydrated electron (solvation channel) and an electron attachment on the aqueous cadmium ion (reduction channel). The minor channels due to the relaxation of excited CTTS and electron−atom pairs (eqs 2b, 2c) are not reported on the figure. (B) Ultrafast dynamics of early electronic trajectories discriminated in aqueous sodium chloride solution following the femtosecond UV excitation of an electron donor (Cl^-).

and solvation times of an excess electron in the aqueous bulk. In $CdCl_2$ solution, these times characterize the nonreactive fraction of IR prehydrated electron $(e^-_{IR})_{p\rightarrow s}$ relaxing toward the ground state of hydrated electron (eq 1b). As previously discriminated in aqueous magnesium chloride solution, the two minor channels assigned to CTTS** and electron−atom pairs (eq 2b,c) are included in the kinetic model of aqueous $CdCl_2$ solution. In order to avoid numerous adjustable parameters of our IR kinetic model at very short time, these minor nonreactive electronic dynamics are kept similar in presence of Mg^{2+} and Cd^{2+}. Tables 1 and 2 report the adjusted parameters obtained from IR spectroscopy of short-lived p-state electrons in aqueous magnesium and cadmium chloride solutions at 294 K.

3.3. IR and Visible Spectroscopy of a Prehydration Electron Transfer Reaction. For different temporal windows (2, 4, and 6 ps) the key points we have investigated concern (i) the dynamics of the prehydration reaction between e^-_{IR} and $Cd^{2+}(T_{Reac})$ and (ii) the discrimination of an early partition leading either to the p → s transition of trapped electrons or the presolvation reduction of aqueous Cd^{2+} (Figures 1−3). At very short time ($t < 2$ ps), the relative spectral contributions (RSC) of two subpicosecond IR electron trajectories (eq 1a,b) is defined by the following expression:

$$\mathrm{RSC}_{ni}^{\omega T} = \alpha_i^{\omega T}/\sum \alpha_i^{\omega T} = \sigma_i^{\omega T} P_i n_i^* \qquad (7)$$

In this expression, the adjusted parameter $\alpha i^{\omega T}$ represents the relative contribution of a given population of IR electrons; $\sigma_i^{\omega T}$ is the cross section of IR electrons involved in the channel i and P_i the probability of this IR channel i. The early branching ratio occurring between reactive and nonreactive IR electron trajectories has been expressed by eq 8:

$$\frac{\alpha_{[e-IR]Reac}^{\omega T}}{\alpha_{[e-IR]p\rightarrow s}^{\omega T}} = \frac{\sigma_{[e-IR]Reac}^{\omega T} P_{Reac}}{\sigma_{[e-IR]p\rightarrow s}^{\omega T} P_{p\rightarrow s}} \qquad (8)$$

If $\sigma^{0.99\ eV}\,[e^-_{IR}]_{Reac}$ equals $\sigma^{0.99\ eV}\,[e^-_{IR}]_{p\rightarrow s}$, the IR branching ratio becomes

$$\frac{P_{Reac}}{P_{p\rightarrow s}} = \frac{\alpha_{[e-IR]Reac}^{\omega T}}{\alpha_{[e-IR]p\rightarrow s}^{\omega T}} \qquad (9)$$

Consequently, the probability P_{Reac} characterizing the reactive IR electron channel ($[e^-_{IR}]_{Reac}$) is defined by the following equation:

$$P_{Reac} = 1 - P_{p\rightarrow s} = 1 - \frac{\alpha_{[e-IR]p\rightarrow s}^{\omega T}}{(\alpha_{[e-]IR\ Reac}^{\omega T} + \alpha_{[e-]IRp\rightarrow s}^{\omega T})} \qquad (10)$$

From computed fits of experimental data performed at 0.99 eV, the expression 10 allows one to calculate an early partition between ultrafast electronic dynamics in term of a probability ratio (Table 1). In $CdCl_2$ solutions, the most important results concern the behavior of the IR p-like electron. The high branching ratio ($P_{Reac}/P_{p\rightarrow s}$) characterizes a prehydration electron transfer reaction with Cd^{2+}. This prevailing IR electronic dynamics ($T_{Reac} = 140 \pm 20$ fs) corresponds to an ultrafast univalent reduction of aqueous Cd^{2+} by IR presolvated electrons (eq 1a). The probability of this prehydration electron transfer is 10 times higher than the solvation channel and its frequency rate ν_{ET} equals $7 \times 10^{12}\ s^{-1}$ against $3.3 \times 10^{12}\ s^{-1}$ for the p → s transition of IR excited hydrated electrons (Figure 1, Table 1). As previously seen by eq 10, the branching ratio between reactive and nonreactive IR electronic channels is not equivalent to a simple expression between nonreactive and reactive electron dynamics (T_2/T_{Reac}). This result represents the first time-resolved spectroscopic evidence of an ultrafast univalent reduction reaction of an aqueous divalent ion by p-state of short-lived IR electrons. In this way, Figure 3B underlines the significant difference between this ultrafast univalent reduction dynamics of Cd^{2+} (T_{reac}) and the time dependence (T_2) of p → s transition within the electron hydration channel (eq 1b). This electron hydration dynamics remains independent of the Mg^{2+}/Cd^{2+} substitution. However, its probability is significantly lowered by the presence of Cd^{2+} (Table 1).

The ultrafast prehydration electron reaction with Cd^{2+} influences the IR signal amplitude (S_{max}) determined at the femtosecond time scale (Figure 2). In order to explain carefully these important results, we have performed a comparison between the experimental IR S_{max} and the computed signal amplitude at $t = 300$ fs ($MgCl_2$) and $t = 200$ fs ($CdCl_2$). This computed analysis has been extended to the long-lived IR component observed at $t = 4$ ps (Figures 1 and 2B, and Table 2). The calculated $S_{max}^{\omega T}$ is defined by the eq 11:

$$S_{max}^{\omega T} = \sum_i \alpha_i^{\omega T} n_i^{\tau S_{max}} \qquad (11)$$

In this expression, $\alpha_i^{\omega T}$ represents the relative spectral contri-

TABLE 2: Computed Spectral Contributions of Electronic States to Experimental IR Absorption Signals (0.99 eV) at τS_{max} and $\tau = 4$ ps following the Femtosecond UV Excitation of Aqueous Magnesium and Cadmium Chloride Solutions ($[H_2O]/[XCl_2] = 110$, X = Mg or Cd)

signal analysis	$\tau S_{max} = 300$ fs Mg^{2+}	$\tau S_{max} = 200$ fs Cd^{2+}	$\tau = 4$ ps Mg^{2+}	$\tau = 4$ ps Cd^{2+}
CTTS**	0.004	0.01	0	0
$(e^-_{IR})_{p\rightarrow s}$	0.124	0.01	0	0
$(e^-_{IR})_{Reac}$	0	0.07	0	0
$(Cl{:}e^-)_{pairs}$	0.025	0.014	0.001	0.0002
e^-_{hyd}	0.013	0.003	0.018	0.0058
$(e^-\cdots X^{2+})_{hyd}$	0.0001	0	0.0003	0
calculated signal (0.99 eV) (au)	0.166	0.107	0.019	0.006
experimental signal (0.99 eV) (OD)	0.0168	0.0098	0.0020	0.00062
$S^{0.99\ eV}_{Mg2+}/S^{0.99\ eV}_{Cd2+}$				
model		1.55		3.16
experiment		1.71		3.25

bution of IR absorption electronic states and $n_i^{\tau S_{max}}$ the computed levels of different electronic states at $t_{S_{max}}$. The computed analysis for $MgCl_2$ and $CdCl_2$ solutions capture the experimental IR measurements of S_{max} at $t_{S_{max}}$. The main Mg^{2+}/Cd^{2+} substitution effects are due to $\{e^-_{IR}\}_{p\rightarrow s}$ in $MgCl_2$ and to $\{e^-_{IR}\}_{Reac}$ in $CdCl_2$ (Table 2). When the metal cation exhibits a high electronic affinity (Cd^{2+} vs Mg^{2+}), the results emphasize the existence of an early partition from excited electron donor between the prevailing reactive channel ($\{e^-_{IR}\}_{Reac}$) and the minor electron solvation channel ($\{e^-_{IR}\}_{p\rightarrow s}$). It can be observed that the low spectral contribution of minor electronic channels (CTTS** and {electron−Cl}pairs) cannot influence the dramatic IR S_{max} decrease observed in aqueous $CdCl_2$ solution. At longer time ($\tau = 4$ ps), the incomplete recovery of the IR signal is due to the contribution of the low-energy tail of hydrated electron ground state (s-like state). In aqueous $CdCl_2$ solution, this long-lived IR contribution is lowered (Figure 1 and Table 2).

The subpicosecond competition that occurs between the energy gap relaxation from the first excited state to the ground state of e^-_{hyd} (e^-_S) and the ultrafast electron attachment on aqueous Cd^{2+} (eq 1) modulates the IR signal rise time at 0.99 eV. This early one-electron reduction of $(Cd^{2+})_{aq}$ by the p-state of prehydrated electron would impede an efficient electron hydration channel (Figure 3A). In order to verify this important point raised from the analyses femtosecond IR investigations, we have performed ultrafast visible spectroscopy of fully relaxed electron (ground states of hydrated electrons). The data reported in Figure 4 exhibit a dramatic Mg^{2+}/Cd^{2+} substitution effect on the amplitude of the visible absorption signal at 1.77 eV (700 nm). We have focused our attention on the absorption signal rise time and S_{max} values. Although the apparent signal rise time of normalized curves remains similar in presence of Mg^{2+} and Cd^{2+} (Figure 4B), the early signal behavior and spectral contributions of transient and relaxed electronic states are different (Table 3). The best computed fits of the visible signal rise time include the characteristic times determined in the IR (T_1, T_1', T_2, T_{Reac}). In aqueous $MgCl_2$ solution, within the absorption signal rise time ($\tau = 520$ fs), small contributions of transient $(e^-_{IR})_{p\rightarrow s}$ and electron−chlorine atom pairs overlap with those of hydrated electrons (ground states). In agreement with previous femtosecond spectroscopic investigations of aqueous sodium chloride solutions,[15,42,52,53] two fully relaxed electronic configurations (e^-_{hyd}) and polaron like state $(e^-...Mg^{2+})_{hyd}$ mainly contribute to $S^{1.77eV}_{max}$ (Table 3). For $\tau = 1.48$ ps, 78% of the photoinduced absorption signal is due to the spectral contribution of the hydrated electron gound state (s state) and 17% to the polaron like state $(e^-...Mg^{2+})_{hyd}$. This long-lived electronic state corresponds to a short-range coupling between

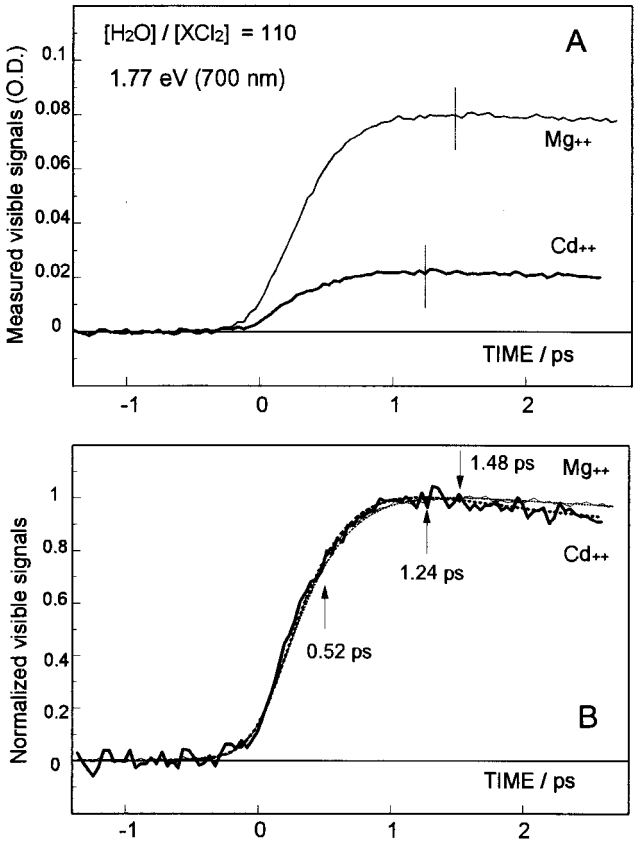

Figure 4. Influence of ultrafast reactivity of IR p-state excited electron (prehydrated electron) with an aqueous divalent cadmium ion on the signal rise time and amplitude at 1.77 eV (700 nm) following the UV femtosecond excitation of aqueous solutions ($[H_2O]/[XCl_2] = 110$, X = Mg or Cd). In magnesium chloride solution, the visible absorption signal is mainly due to the contribution of the ground state of hydrated electron (s state) and to polaron-like state $(e^-...Mg^{2+})_{hyd}$. A Mg^{2+}/Cd^{2+} substitution decreases significantly the amplitude of the absorption signal (A). For the normalized signals (B), the dashed lines represent the computed best fits of the experimental traces. The vertical lines indicate the position of τS_{max} and the arrows the temporal delay (τ) used for the calulations of spectral contributions reported in Table 3.

a s state of electron trapped in the vicinity of hydrated Mg^{2+}. This relaxed state is linked to a complete adiabatic electron photodetachment process from electron−chlorine atom pairs (eq 12) whose the spectral signature peaks in the near-IR.[42,52]

$$(Cl^-, Mg^{2+})_{aq} + 2h\nu \underset{330\ fs}{\rightleftharpoons} (Cl{:}e^-)_{aq}, (Mg^{2+})_{aq} \xrightarrow{t = 730\ fs} (e^-\cdots Mg^{2+})_{aq}, Cl \quad (12)$$

TABLE 3: Computed Spectral Contributions of Electronic States to Experimental Visible Absorption Signals (1.77 eV) at τ = 520 fs and τS_{max} following the Femtosecond UV Excitation of Aqueous Magnesium and Cadmium Chloride Solutions ([H_2O]/[XCl_2] = 110, X = Mg or Cd)

signal analysis	τ = 520 fs		τS_{max} = 1.48 ps	τS_{max} = 1.24 ps
	Mg^{2+}	Cd^{2+}	Mg^{2+}	Cd^{2+}
CTTS**	0	0	0	0
$(e^-_{IR})_{p\rightarrow s}$	0.024	0.0001	0.001	0.00001
$(e^-_{IR})_{Reac}$	0	0.0008	0	0.00002
$(Cl{:}e^-)_{pairs}$	0.087	0.0242	0.035	0.0127
e^-_{hyd}	0.388	0.122	0.564	0.177
$(e^-\cdots X^{2+})_{hyd}$	0.047	0	0.121	0
calculated signal (1.77 eV) (au)	0.546	0.147	0.721	0.189
experimental signal (1.77 eV) (OD)	0.063	0.017	0.080	0.021
$S^{1.77\ eV}_{Mg2+}/S^{1.77\ eV}_{Cd2+}$				
model	3.71		3.81	
experiment	3.70		3.81	

In the presence of hydrated Cd^{2+}, this adiabatic electronic trajectory does not occur and 94% of $S^{1.77eV}_{max}$ (τ = 1.24 ps) involves the contribution of fully hydrated electron (e^-_{hyd}). Due to a Mg^{2+}/Cd^{2+} substitution, the decrease of the experimental $S^{1.77eV}_{max}$ (Figure 4A) agrees with the fact that the prevailing fraction of IR presolvated electron reacting with aqueous Cd^{2+} (P_{reac} = 0.91) does not contribute to an electron hydration channel (Figure 3A, Tables 1,3).

At this stage of our analysis, we have tentatively defined a short-time (C_{37}) value of aqueous cadmium solution considering (i) a direct reaction the IR p-state of hydrated electron and the ionic acceptor (eq 1a), and (ii) a cadmium ion concentration dependence on the short-time level of fully hydrated electrons as previously shown by subnanosecond pulse radiolysis experiments.[45,47,48,49] On our assumption, the influence of prehydration electron transfer on the early level of ground state of hydrated electron would obeyed to the following relation:

$$\frac{S^{\omega T}_{[e^-_S]_{Cd^{2+}}}(\tau)}{S^{\omega T}_{[e^-_S]_{Mg^{2+}}}(\tau)} = \exp^{-[Cd^{2+}]/C_{37}(\tau)} \Rightarrow C_{37}(\tau) = \frac{0.5}{\ln\left(\frac{S^{\omega T}_{[e^-_S]_{Mg^{2+}}}(\tau)}{S^{\omega T}_{[e^-_S]_{Cd^{2+}}}(\tau)}\right)} \quad (13)$$

In this equation, $S^{\omega T}_{[e-s]X^{2+}}(\tau)$ represents the short-time signal contribution of fully relaxed electron (s-state and polaron-like state) to the visible signal (1.77 eV) in the presence of aqueous cadmium or magnesium ion. For different time delay between pump and probe beams, $S^{\omega T}_{[e-s]X^{2+}}(\tau)$ is defined by an equation similar to eq 11 (eq 14). The second part of eq 14 represents the contribution of polaron-like states. In cadmium chloride solutions, this part equals 0.

$$S^{\omega T}_{[e\cdot S]_{X^{2+}}}(\tau) = \alpha^{\omega T}_{(e\cdot s)} \cdot n_{(e\cdot s)}(\tau) + \alpha^{\omega T}_{(e^-\cdots X^{2+})_s} \cdot ns_{(e^-\cdots X^{2+})_s(\tau)} \quad (14)$$

The present work permitting us to determine the time dependence of spectral contributions of fully relaxed states of electron, eqs 13 and 14 have been used for different time delay (τ = 0−2 ps). The results on the time dependence of the C_{37} value are reported in Figure 5. When the analysis are performed around τS_{max} (1.24 ps for Cd^{2+} and 1.48 ps for Mg^{2+}), we can emphasize the existence of a good agreement between the C_{37} values determined from the measured $S^{1.77eV}_{max}$ and expression 13 ($C_{37} \sim 0.37 \pm 0.05$). At very short time, i.e., during the visible signal rise time, small fluctuations of the calculated C_{37} occur (Figure 5). In any case, these C_{37} estimates are in agreement with previous subnanosecond pulse radiolysis data obtained for different ionic concentrations (C_{37} of aqueous Cd^{2+} = 0.38).[47−49]

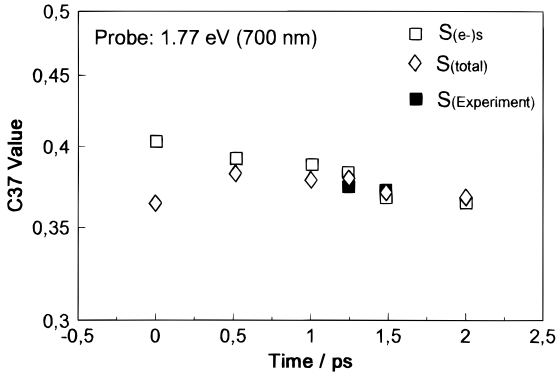

Figure 5. Time dependence of C_{37} value of aqueous cadmium solution (R = 110) following femtosecond photoinduced electron transfers probe at 1.77 eV (700 nm). $S(e^-)_s$, S(total) correspond to calculated C_{37} value from spectral contribution of fully solvated electron and total electronic states, respectively. The C_{37} values directly obtained from measured absorption signals are represented by black squares.

3.4. Reactive Counterion Concentration Effect on Ultrafast Electron Dynamics. Contrary to subnanosecond pulse radiolysis investigations on concentrations dependence of fast electron scavenging processes,[47−49] the aim of our femtosecond laser spectroscopic study is mainly devoted to the direct determination of ultrafast electronic trajectories and their influence on transient IR and visible signal amplitudes. These short time spectroscopic determinations being complex by themselves, the investigation of time dependence of electric field effects on IR electronic dynamics represent another research challenge for the future. However, let us consider preliminary investigations of Cd^{2+} concentrations effects on ultrafast IR and visible spectroscopy of prehydration electron transfer.

Figure 6 reports IR and visible results obtained for three $CdCl_2$ concentrations (0, 0.3, and 0.5 M). At 0.3 M (R = 183), the IR signal dynamics (rise time and relaxation) remains similar to those obtained for a molecular ration of 110 (Cd^{2+} = 0.5 M). This result would indicate that the dynamics of the prehydration electron transfer involving excited p-like electron (eq 1a) is not directly dependent of the macroscopic parameter (ionic concentration) and that short-time electric field effects on electron attachment (sceening effects) cannot be interpreted in the framework of a simple pseudo-first order approach. A Cd^{2+} concentration dependence on $S^{\omega T}_{max}$ can be observed from simultaneous IR and visible spectroscopic investigations (Figure 6B). The exponential regression reported in the figure is not senseless if we consider, as previously discussed, a Cd^{2+}

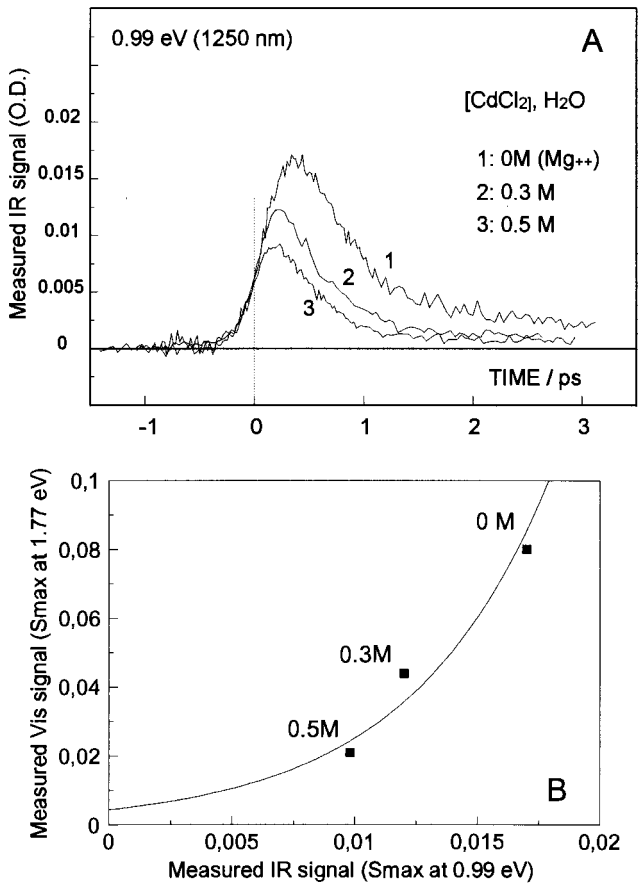

Figure 6. (A) Influence of cadmium concentration on measured IR absorption signal (0.99 eV), following femtosecond UV excitation of aqueous cadmium chloride solutions at 294 K. (B) For different cadmium concentrations, the relationship between transient absorption signals ($S^{\omega T}_{max}$) simultaneously measured at 0.99 and 1.77 eV. The smooth line represents an exponential regression between measured IR and visible signals: $S^{1.77\ eV}_{max} = 0.0439 \exp(174.4 S^{0.99\ eV}_{max})$.

concentration dependence on the transient signal ratio ($S_{Cd^{2+}}/S_{Mg^{2+}}$) at 1.77 eV (eqs 13 and 14, Table 3). This significant Cd^{2+} concentration effect on IR and visible signals agrees with our IR kinetic model (Figure 3A) and permits us to conclude that the direct IR discrimination of a prehydration univalent reduction of Cd^{2+} occurs faster than the nonadiabatic p $\rightarrow$ s radiationless transition of excited electron relaxation (eq 1, Figure 3, Table 1).

The characteristic time (T_{Reac}) of this prehydration Cd^{2+} reduction by a quantum particule (p-state electron) is not directly dependent on the Cd^{2+} concentration within the range 0.3−0.5 M. Consequently, a complete understanding of excited p-state electron reactivity at very short time ($\tau \ll 1$ ps) and at the microscopic level cannot be only obtained from investigations on counterion concentration effects. One major reason is that the prehydration electron transfer is likely dependent on ion-pair distribution function, ion−solvent correlation functions, and short-range ordering of water molecules around isolated anions, cations, or ion pairs. Previous concentrations effects on femtosecond spectroscopy of aqueous electrolyte solution with nonreactive counterions have shown that the global signal rise time in the visible spectral range 2.3−1.72 eV is highly dependent on the dynamics of multiple electronic channels: electron hydration in bulk water, transient electron detachment in the vicinity of polarizable chlorine atoms, and early geminate recombination processes between hydrated electron ground state and its chlorine parent.[15,38,42,52,53,55] In the visible region, a significant fraction of the absorption signal can be due to fully relaxed hydrated electron whose transient electronic precursors (electron−Cl atom pairs) exhibit a spectral signature in the near-IR (~1.41 eV). Simultaneously, the relative spectral contribution of electronic trajectories involving IR p-state electrons is decreased.[15,52,55] In the present work, pioneering femtosecond IR and visible spectroscopy of complex ionic concentration effects on prehydration electron reaction provides guidance for further research on ultrafast electron transfer with reactive counterions or charged electron acceptors. The prediction of a resting visible signal when the IR signal equals 0 will be interesting to consider (Figure 6B). However, technical limitations linked to careful discrimination of small IR signals (OD < 0.005) in concentrated solutions with reactive counterions would be overcome.

Taking into account the counterion concentration dependence on spectral contribution of transient electron−Cl atom pairs,[52] the complete understanding of dynamical electric field effects on prehydration redox reaction in electrolyte solution needs to develop multiwavelength analysis of transient electronic dynamics within the spectral range 2.3−0.99 eV. Such experimental work would permit to determine the respective influence of reactive IR prehydration electron transfer, p $\rightarrow$ s radiationless transition of prehydrated electrons, and near-IR dynamics of electron−chlorine atom pairs on nonadiabatic and adiabatic electron hydration channels. By exploring Cd^{2+} concentration effects in the near-IR, we hope to understand how highly polarizable Cl atoms favor ultrafast univalent reduction of aqueous Cd^{2+} ions from transient electron−chlorine atom pairs and impede the formation of short-lived polaron-like states. Regarding the conclusions of recent ESR studies and ab initio calculations on the chlorine atom interaction with water molecules,[56] we should wonder whether the formation of three-electron $2\sigma/1\sigma^*$ bonding assists an ultrafast electron transfer from a photoinduced electron−Cl atom pair to the hydrated ionic acceptor.

4. Concluding Remarks

The present work devoted to femtosecond IR spectroscopy of electron dynamics in aqueous $MgCl_2$ and $CdCl_2$ solutions provides insight into significant counterion effects on early partition between reactive (prehydration redox reaction) and nonreactive electron trajectory (electron hydration). Our simultaneous visible and IR spectroscopic studies permit us to well capture the Mg^{2+}/Cd^{2+} substitution effect on the amplitude and the absorption signal dynamics due to either nonequilibrium electronic states (IR presolvated electron) or fully relaxed states (s state of hydrated electron and polaron like state) whose the spectral band peaks in the red spectral region.

In order to focus our attention on the careful discrimination of complex spectroscopic results devoted to ultrafast prehydration electron transfer in aqueous ionic solution, the femtosecond spectroscopic experiments have been mainly performed at a given counterion concentration ($R = 110$) for which there is good visible and IR signal noise ratios. The primary step of a prehydration one-electron reduction of a divalent cation (Cd^{2+}) occurs with a characteristic time of 140 fs and involves short-lived nonequilibrium electron−solvent couplings in the vicinity of the bivalent metallic ion (Figure 7). In aqueous cadmium chloride solution, the elementary redox process exhibits a probability 10 times higher than the electron solvation channel and is totally achieved in less than 1×10^{-12} s. Our femtosecond IR spectroscopic data cannot be captured by recent nonadiabatic quantum simulations of an excess electron relax-

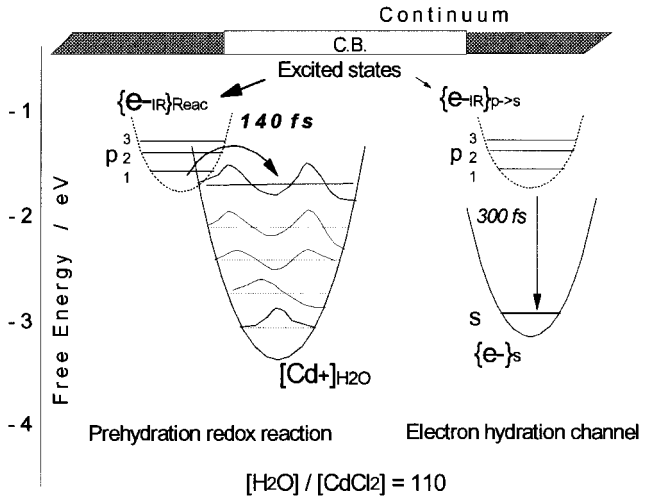

Figure 7. Energy level diagram of two IR electronic dynamics in aqueous cadmium chloride solutions ($R = 110$). The prevailing IR channel corresponds to an ultrafast prehydration redox reaction of aqueous cadmium ions with $\{e^-_{IR}\}_{Reac}$. A slower nonreactive electronic channel involving a radiationless transition ($\{e^-_{IR}\}_{p\rightarrow s}$) leads to the formation of a ground state of the hydrated electron (e^-_s).

ation within a neutral bath of water molecules. Further computer simulations of prehydration electron transfer in ionic solutions would include quantum model of flexible molecules, and ab initio molecular dynamics on electronic structure of aqueous solution containing ions.[11,57−63] Moreover, interionic energy transfer, short-range solvent polarization effects, and detailed treatment of ionic hydration with adequate nonempirical potentials are also required.[64−68]

The understanding of vibronic couplings in electrolyte solutions needs to determine whether their dynamics are dependent on intracomplex structural changes of the cavity of p state electron and/or the distortion of the first hydration shell of cadmium ion. Additional experimental works are envisaging the effects of solvent cavity size fluctuations and the role of high-frequency vibrational modes of solvent molecules around cations as rate-limiting steps of ultrafast IR presolvation reactions in polar solutions.[69] These IR spectroscopies of prehydration electron transfers provide guidance for further theoretical investigations on solvation effects in transition state theory, mainly on nonlinear response of solvent molecules to an electronic reorganization of small reactants (ionic donors and acceptors). This point represents an interesting and worthwhile problem for furture experimental investigations on prethermal chemistry in dilute or concentrated ionic solutions.

Acknowledgment. This work was supported by the GDR 1017 of the CNRS (France) and the Commission of the European Communities.

References and Notes

(1) Mukamel, S. *Annu. Rev. Phys. Chem*. **1990**, *41*, 647 and references therein. See also the special issue of *J. Opt. Soc. Am.* **1990**, *B 7*. Wang, N.; Chernyak, V.; Mukamel S. *J. Chem. Phys*. **1994**, *100*, 2465. *Principles of nonlinear optical spectroscopy*; Mukamel, S., Ed.; Oxford University Press: London, 1995. Potter, E. D.; Liu, Q.; Zewail, A. H. *Chem. Phys. Lett.* **1992**, *200*, 605. Zewail, A. H. *J. Phys. Chem*. **1996**, *100*, 12701 and references therein.

(2) *Advances in multiphoton processes and spectroscopy*; Lin, S. H., Ed.; World Scientific: Singapore 1989; p 175. *Applications of time-resolved optical spectroscopy*; Bruckner, V., Feller, K. H., Grummt, U. W., Eds.; Elsevier: New York, 1990. *Ultrashort Laser Pulse Phenomena;* Diels, J. C., Rudolph, W., Eds.; Academic Press: San Diego, CA, 1996.

(3) *Femtosecond Chemistry*; Manz, J., Woste, J. L., Eds.; VCH, Heidelberg, 1995.

(4) Jonas, D. M.; Bradforth, S. E.; Passino, S. A.; Fleming, G. R. *J. Phys. Chem*. **1995**, *99*, 2594.

(5) Bratos, S.; Leicknam, J. C. *Chem. Phys. Lett*. **1996**, *261*, 117; *J. Chim. Phys*. **1996**, *93*, 1737.

(6) Nibbering, E. J.; Wiersma, D. A.; Duppen, K. *Phys. Rev. Lett*. **1991**, *66*, 2462. Duppen, K.; de Haan, F.; Nibbering, E. T. J.; Wiersma, D. A. *Phys. Rev. A* **1993**, *47*, 5120.

(7) Bagchi, B. *Ann. Rev. Phys. Chem*. **1989**, *40*, 115. Bagchi, B.; Chandra, A. *Adv. Chem. Phys*. **1991**, *80*, 1. Roy, S.; Bagchi, B. *J. Chem. Phys*. **1993**, *99*, 1310, 3139, 9938. Roy, S.; Bagchi, B. *Chem. Phys*. **1994**, *183*, 207. Nandi, N.; Roy S.; Bagchi B. *J. Chem. Phys.* **1995**, *102*, 1390. Ravichandran, S.; Roy, S.; Bagchi, B. *J. Phys. Chem*. **1995**, *99*, 2489. Biswas, R.; Bagchi, B. *J. Phys. Chem.* **1996**, *100*, 1238.

(8) Jortner, J.; Bixon, M. *J. Chem. Phys*. **1988**, *88*, 167. Rips, I.; Klafter, J.; Jortner, J. *J. Chem. Phys*. **1988**, *88*, 3246. Stell, G.; Zhou, Y. *J. Chem. Phys.* **1989**, *91*, 4869, 4879, 4885. Rips, I.; Pollack, E., *J. Chem. Phys*. **1995**, *103*, 7912. Rips, I. *Chem. Phys. Lett*. **1995**, *245*, 79; *J. Chim. Phys*. **1996**, *93*, 1591.

(9) Hynes, J. T. *Annu. Rev., Phys. Chem.* **1985**, *36*, 573. Kim, H. J.; Hynes, J. T. *J. Phys. Chem.* **1990**, *94*, 2736. Keirstead, W. P.; Wilson, K. R.; Hynes, J. T. *J. Chem. Phys*. **1991**, *95*, 5256. Van der Zwan, G.; Hynes J. T. *Chem. Phys.* **1991**, *152*, 169.

(10) Rossky, P. J. *J. Opt. Soc. Am*. **1990**, *B7*, 1727. Webster, F.; Rossky, P. J.; Friesner, R. A. *Comput. Phys. Commun.* **1991**, *63*, 494. Webster, F.; Schnitker, J.; Friedrich, M. S. M.; Friesner, R. A.; Rossky, P. J. *Phys. Rev. Lett*. **1991**, *66*, 3172. Webster, F.; Wang, E. T.; Rossky, P. J.; Friesner, R. A. *J. Chem. Phys*. **1994**, *100*, 4835.

(11) Sprik, M.; Klein, M. L. *J. Chem. Phys*. **1988**, *89*, 7556. Sprik, M. *J. Phys. Chem*. **1991**, *95*, 2283. Laasonen, K.; Sprik, M.; Parrinello, M.; Car, R. *J. Chem. Phys*. **1993**, *99*, 9080. Tuckerman, M.; Laasonen, K.; Sprik, M.; Parrinello, M. *J. Phys. Chem*. **1995**, *99*, 5749; *J. Chem. Phys*. **1995**, *103*, 150.

(12) Fonseca, T.; Ladanyi, B. *J. Phys. Chem*. **1991**, *95*, 2116; *J. Mol. Liq*. **1994**, *60*, 1. Ladanyi, B. M.; Stratt, R. M. *J. Phys. Chem*. **1995**, *99*, 2502; **1996**, *100*, 1266.

(13) *The Chemical Physics of Solvation, Parts A, B, C*; Dogonadze, R. R., Kalman, E., Kornyshev, A. A., Ulstrup, J., Eds.; Studies in Physical and Theoretical Chemistry, 38; Elsevier: New York, 1988. Bursulaya, B. D.; Zichi, D. A.; Kim, H. J. *J. Phys. Chem*. **1996**, *100*, 1392.

(14) Newton, M. D. *Chem. Rev*. **1991**, *91*, 767. Marcus, R. A., *Rev. Mod. Phys*. **1993**, *65*, 599. Lami, A.; Santoro, F. *J. Chem. Phys*. **1997**, *106*, 94.

(15) *Ultrafast Reaction Dynamics and Solvent Effects*; Gauduel, Y., Rossky, P. J., Eds.; AIP Press: New York, 1994; Vol. 298. See also a recent Special Issue: Elementary Chemical Processes in Liquids and Solutions, *J. Chim. Phys*. **1996**, *93*, 1577-1938.

(16) *Ultrafast dynamics of chemical systems*; Simon, J. D., Ed.; Kluwer: Dordrecht, 1994.

(17) Maroncelli, M.; Fleming, G. R. *J. Chem. Phys.* **1988**, *89*, 875. Maroncelli, M. *J. Chem. Phys*. **1991**, *94*, 2084. Papazyan, A.; Maroncelli, M. *J. Chem. Phys.* **1993**, *98*, 6431. Horng, M. L.; Gardecki, J. A.; Papazyan, A.; Maroncelli, M. *J. Phys. Chem*. **1995**, *99*, 17311; *J. Chem. Phys*. **1995**, *102*, 2888.

(18) Yoshihara, K.; Tominaga, K.; Nagasawa, Y. *Bull. Chem. Soc. Jpn*. **1995**, *68*, 696.

(19) Stratt, R. M.; Cho, M. *J. Chem. Phys*. **1994**, *100*, 6700; Stratt, R. M.; Maroncelli, M. *J. Phys. Chem*. **1996** *100*, 12981.

(20) Raineri, F.; Resat, H.; Perng, B. C.; Hirata, F.; Friedman, H. *J. Chem. Phys*. **1994**, *100*, 1477.

(21) Voth, G. A.; Hochstrasser, R. M. *J. Phys. Chem*. **1996**, *100*, 13034.

(22) Day, P. N.; Jensen, J. H.; Gordon, M. S.; Webb, S. P.; Stevens, W. J.; Krauss, M.; Garmer, D.; Basch, H.; Cohen, D. *J. Chem. Phys*. **1996**, *105*, 1968.

(23) Walrafen, G. E.; Hokmabadi, M. S.; Yang, W. H. *J. Chem. Phys*. **1986**, *85*, 6964.

(24) Sasai, M. *J. Chem. Phys*. **1990**, *93*, 7329.

(25) Mizoguchi, K.; Tominaga, Y. *J. Chem. Phys*. **1992**, *97*, 1961.

(26) Ohmine, I.; Tanaka, H. *Chem. Rev.* **1993**, *93*, 2545.

(27) Cho, M.; Fleming, G. R.; Saito, S.; Ohmine, I. *J. Chem. Phys*. **1994**, *100*, 6672.

(28) Chandler, D.; Leung, K. *Annu. Rev. Phys. Chem*. **1994**, *45*, 557.

(29) Castner, E. W.; Maroncelli, M.; Fleming, G. R. *J. Chem. Phys*. **1987**, *86*, 1090. Castner, E. W.; Fleming, G. R.; Bagchi, B.; Maroncelli, M. *J. Chem. Phys*. **1988**, *89*, 3519.

(30) Barbara, P. F.; Jarzeba, W. In *Advances in Photochemistry*; Volman, D. H., Hammond, G. S., Gollnick, K., Eds.; Wiley-Interscience: New York, **1989**, *15*, 1. Kahlow, M. A.; Jarzeba, W.; Kang, T. J.; Barbara, P. F. *J. Chem. Phys*. **1989**, *90*, 151. In *Structure and Dynamics of Solutions*; Part 4, Studies in Physical and Theoretical Chemistry; Ohtaki, H., Yamatera, H., Eds.; Elsevier: New York, 1992.

(31) Gauduel, Y.; Martin, J. L.; Migus, A.; Antonetti, A. *Ultrafast Phenomena V*; Fleming, G. R., Siegman, Eds.; Springer Verlag: New York,

1986; p 308. Migus, A.; Gauduel, Y.; Martin, J. L.; Antonetti, A.; *Phys. Rev. Lett*. **1987**, *108*, 318.

(32) Long, F. H.; Lu, H.; Shi, X.; Eisenthal, K. B. *J. Chem. Phys.* **1989**, *91*, 4103; *Chem. Phys. Lett*. **1990**, *169*, 165.

(33) Alfano, J. C.; Walhout, P. W.; Kimura, Y.; Barbara, P. F. *J. Chem. Phys*. **1993**, *98*, 5996. Kimura, Y., et al. *J. Phys. Chem*. **1994**, *98*, 3450.

(34) Reuther, A.; Laubereau, A.; Nikogosyan, D. N. *J. Phys. Chem*. **1996**, *100*, 16794.

(35) Sheu, W. S.; Rossky, P. J. *J. Am. Chem. Soc*. **1993**, *115*, 7729.

(36) Borgis, D.; Staib, A. *Chem. Phys. Lett*. **1994**, *230*, 405. Staib, A., Borgis, D. *J. Chem. Phys.* **1995** *103*, 2642; **1996**, *104*, 4776, 9027.

(37) Sheu, W. S.; Rossky, P. J. *Chem. Phys. Lett*. **1993**, *213*, 233. Schwartz, B. J.; Rossky, P. J. *Phys. Rev. Lett*. **1994**, *72*, 3282; *J. Chem. Phys*. **1994**, *101*, 6902, 6917; *J. Phys. Chem*. **1995**, 99, 2953. Schwartz, B. J.; Rossky, P. J. *J. Chem. Phys*. **1996**, *105*, 6997; *J. Phys. Chem*. **1996**, *100*, 1295. Prezhdo, O. V.; Rossky, P. J. *J. Phys. Chem*. **1996**, *100*, 17094.

(38) Pommeret, S.; Antonetti, A.; Gauduel, Y. *J. Am. Chem. Soc*. **1991**, *113*, 9105; *J. Phys. Chem*. **1993**, *97*, 134.

(39) Gauduel, Y.; Berrod, S.; Migus, A.; Yamada, N.; Antonetti, A. *Biochemistry* **1988**, *27*, 2509. Gauduel, Y.; Pommeret, S.; Yamada, N.; Migus, A.; Antonetti, A. *J. Am. Chem. Soc*. **1989**, *111*, 4974.

(40) Gauduel, Y.; Migus, A.; Chambaret, J. P.; Antonetti, A. *Rev. Phys. Appl*. **1987**, *22*, 1755. Gauduel, Y.; Pommeret, S., Migus, A.; Yamada, N.; Antonetti, A. *J. Am. Chem. Soc*. **1990**, *112*, 2925.

(41) Long, F. H.; Shi, X.; Lu, H.; Eisenthal, K. B. *J. Phys. Chem*. **1994**, *98*, 7252.

(42) Gauduel, Y.; Gelabert, H.; Ashokkumar, M. *Chem. Phys*. **1995**, *197*, 167. Gauduel, Y.; Gelabert, H.; Ashokkumar, M. *J. Mol. Liq*. **1995**, *64*, 57.

(43) Akesson, E.; Walker, G. C.; Barbara, P. F. *J. Chem. Phys*. **1991**, *95*, 4188.

(44) Nagasawa, Y.; Yartsev, A. P.; Tominaga, K.; Bisht, P. B.; Johnson, A. E.; Yoshihara, K. *J. Phys. Chem*. **1995**, *99*, 653 and reference therein.

(45) Wolff, R. K.; Bronskill, M. J.; Hunt, J. W. *J. Chem. Phys*. **1970**, *53*, 4211. Wolff, R. K.; Aldrich, J. E.; Penner, T.; Hunt, J. W. *J. Phys. Chem*. **1975**, *79*, 210.

(46) Czapski, G.; Peled, E. *J. Phys. Chem.* **1973**, *77*, 893.

(47) Lam, K. Y.; Hunt, J. W. *Int. Radiat. Phys. Chem*. **1975**, *7*, 317.

(48) Jonah, C. D.; Miller, J. R.; Hart, E. R.; Matheson, M. S. *J. Phys. Chem*. **1975**, *79*, 2705; Jonah, C. D.; Matheson, M. S.; Miller, J. R.; Hart, E. J. *J. Phys. Chem*. **1976**, *80*, 1267; Jonah, C. D.; Miller, J. R.; Matheson, M. S. *J. Phys. Chem*. **1977**, *81*, 1618; Lewis, M. A.; Jonah, C. D. *J. Phys. Chem*. **1986**, *90*, 5367.

(49) Razem, D.; Hamill, W. H. *J. Phys. Chem*. **1977**, *81*, 1625.

(50) Bolton, G. L.; Jha N.; Freeman G. R. *Can. J. Chem*. **1976**, *54*, 1497. Okazaki K.; Freeman G. R. *Can J. Chem*. **1978**, *56*, 2313. *Kinetics of nonhomogeneous processes*; Freeman, G. R., Ed.; Wiley Interscience: New York, 1987.

(51) Tran-Thi, T. H.; Koulkes-Pujo, A. M.; Sutton, J.; Anitoff, O. *Radiat. Phys. Chem*. **1984**, *23*, 77; Tran-Thi, T. H.; Koulkes-Pujo, A. M. *Radiat. Phys. Chem*. **1984**, *23*, 745.

(52) Gelabert, H.; Gauduel, Y. *J. Phys. Chem*. **1996**, *100*, 13993.

(53) Gauduel, Y.; Gelabert, H. *In Photochemistry and Radiation Chemistry*, Wishart, J., Ed.; Adv. Chem. Series; American Chemical Society: Washington, DC, 1998; Vol. 254, p 331.

(54) Gauduel, Y.; Pommeret, S.; Migus, A.; Antonetti, A. *J. Phys. Chem*. **1991**, *95*, 533.

(55) Gauduel, Y.; Sander, M.; Gelabert, H. *J. Mol. Liq*. **1998**, *78*, 111.

(56) Sevilla, M. D.; Summerfield, S.; Eliezer, I.; Rak, J.; Symons, M. C. R. *J. Phys. Chem*. **1997**, *101*, 2910.

(57) Sprik, M.; Klein, M. L.; Watanabe, K. *J. Phys. Chem*. **1990**, *84*, 6483.

(58) Zhu, S. B.; Zhu, J. B.; Robinson, G. W. *Phys. Rev. A* **1991**, *44*, 2602.

(59) Trokhymchuk, A. D.; Holovko, M. F.; Heinzinger, K. *J. Chem. Phys.* **1993**, *99*, 2964. Liu, K.; Loeser, J. G.; Elrod, M. J.; Host, B. C.; Rzepiela, J. A.; Pugliano, N.; Saykally, R. J. *J. Am. Chem. Soc*. **1994**, *116*, 3507.

(60) Sremaniak, L. S.; Perera, L.; Berkowitz, M. L. *J. Chem. Phys*. **1996**, *105*, 3715.

(61) Bhattacharya, I.; Voth, G. A. *J. Phys. Chem*. **1993**, *97*, 11253. Straus, J. B.; Calhoun, A.; Voth, G. A. *J. Chem. Phys.* **1995,** *102*, 529. Lobaugh, J.; Voth, G. A. *J. Chem. Phys*. **1996,** *104*, 2056. Parese, M.; Chawla, S.; Lu, D.; Lobaugh, J.; Voth, G. A. *J. Chem. Phys*. **1997**, *107*, 7428.

(62) Burda, J. V.; Sponer, J.; Hobza, P. *J. Phys. Chem.* **1996**, *100*, 7250.

(63) Ando, K. *J. Chem. Phys*. **1997**, *106*, 116.

(64) Kowall, Y.; Foglia, F.; Helm, L.; Merbach, A. E. *J. Phys. Chem*. **1995**, *99*, 13078.

(65) Blenzen, A.; Foglia, F.; Furet, E.; Helm, L.; Merbach, A. E.; Weber, J. *J. Am. Chem. Soc*. **1996**, *118*, 12777.

(66) Pappalardo, R. R.; Martinez, J. M.; Sanchez Marcos, E. *J. Phys. Chem*. **1996,** *100*, 11748.

(67) Tazaki, K.; Doi, J. *J. Phys. Chem*. **1996,** *100*, 14520.

(68) Maroulis, G. *J. Chem. Phys*. **1998**, *108*, 5432.

(69) Gauduel, Y.; Sander, M.; Gelabert, H., manuscript in preparation.